IOPscience iopscience.iop.org

Home Search Collections Journals About Contact us My IOPscience

Laser Precision Engineering of Glass Substrates

This content has been downloaded from IOPscience. Please scroll down to see the full text.

2004 Jpn. J. Appl. Phys. 43 7102

(http://iopscience.iop.org/1347-4065/43/10R/7102)

View the table of contents for this issue, or go to the journal homepage for more

Download details:

IP Address: 141.161.91.14
This content was downloaded on 24/08/2015 at 02:18

Please note that terms and conditions apply.

Japanese Journal of Applied Physics
Vol. 43, No. 10, 2004, pp. 7102–7106
©2004 The Japan Society of Applied Physics

Laser Precision Engineering of Glass Substrates

Bin LAN[1,2], Ming-Hui HONG[1,2]*, Kai-Dong YE[1], Zeng-Bo WANG[1,2], Shi-Xin CHENG[1,2] and Tow-Chong CHONG[1,2]

[1]*Data Storage Institute, DSI Building, 5 Engineering Drive 1, Singapore 117608, Republic of Singapore*
[2]*Department of Electrical and Computer Engineering, National University of Singapore, Singapore 117576, Republic of Singapore*

(Received October 23, 2003; accepted June 16, 2004; published October 8, 2004)

The precise laser microfabrication of glass is a very challenging task due to the stress-induced microcracks generated during laser ablation. In this paper, the results of high-quality glass microfabrication by low-energy Nd:YAG laser (355 nm, 30 ns) ablation and pocket scanning are presented. Pocket scanning involves the scanning of a laser beam along parallel overlapped paths with the last path forming structural edge, while conventional direct scanning involves the scanning of a beam just along single path to obtain the structure edge. It is found that cracks that formed around the edges by pocket scanning are significantly reduced in size compared with those formed by laser direct scanning. Minimum crack sizes of less than 10 μm have been obtained at optimized parameters. Ablation depth is also enhanced greatly by pocket scanning; it increases almost linearly with laser fluence and the number of scanning loops. There is no saturation of ablation depth as observed in laser direct scanning. This technique has high potential applications in glass precision engineering.
[DOI: 10.1143/JJAP.43.7102]

KEYWORDS: laser ablation, glass, pocket scanning method, cracks, ablation depth

1. Introduction

Glass microdevices have numerous potentials in analytical chemistry, biotechnology and microelectronics because of the excellent mechanical properties, chemical stability and transparent nature of glass. Glass microstructure fabrication is the first step to fulfilling glass applications.[1)] Current mechanical and chemical methods for glass microfabrication are beset with problems such as poor fabrication quality and the use of toxic agents. The development of novel microfabrication techniques is in strong demand in various industries. Pulsed laser ablation is a powerful microfabrication tool attributed to its use of a small beam spot size with a high localized energy.[2)] However, due to the high band-gap and low thermal conductivity of glass, the microcracks generated from thermal stress affect the reliability and quality of the microstructures formed by laser ablation.[3)] Crack-free glass microfabrication is a very challenging task in laser precise engineering.

Thus far, different types of lasers have been proposed and studied for glass microfabrication; these include the CO_2 laser,[4)] excimer laser,[5)] Nd:YAG laser,[6)] F_2 laser[7)] and ultrafast laser.[8)] The drawbacks of the CO_2 laser are that it provides a relatively large beam spot and causes severe thermal effects due to its long wavelength. The use of excimer laser suffers from the high running and maintenance cost. The studies of glass microfabrication using advanced F_2 and ultrafast lasers have obtained excellent results, but the extensive application of these lasers is still limited by their cost and stability problems. The Nd:YAG laser is a low-cost light source for industrial applications. However, since the wavelengths of most Nd:YAG lasers are in the region of transparency for glass (300–2500 nm),[9)] Nd:YAG laser ablation of glass requires a high laser fluence and causes many microcracks due to the diffusion of excess energy and thermal effects. A new method of reducing the number of microcracks generated during laser ablation would enhance the possible use of Nd:YAG lasers in glass microfabrication to meet the industrial requirement for a good profit-performance index.

In this paper, we used pocketing scanning to produce microstructures on glass. Pocket scanning in computer-assisted manufacturing (CAM) is defined as the "parallel overlapped scanning of paths". A low-energy diode-pumped solid-state (DPSS) Nd:YAG laser (355 nm, 30 ns) with a computer-generated laser scanning path was employed. The number of microcracks formed around the ablated grooves in pocket scanning was reduced significantly compared with that produced in laser direct scanning. Ablation efficiency and edge quality were measured and compared between direct scanning and pocket scanning under various combinations of processing parameters. Precise glass microstructures were fabricated with the optimized setting of laser processing parameters.

2. Experimental

The experimental setup for laser microfabrication is schematically illustrated in Fig. 1. The laser employed in this work was a third-harmonic DPSS Nd:YAG laser (Coherent AVIA 355-1500) with the TEM_{00} mode. The

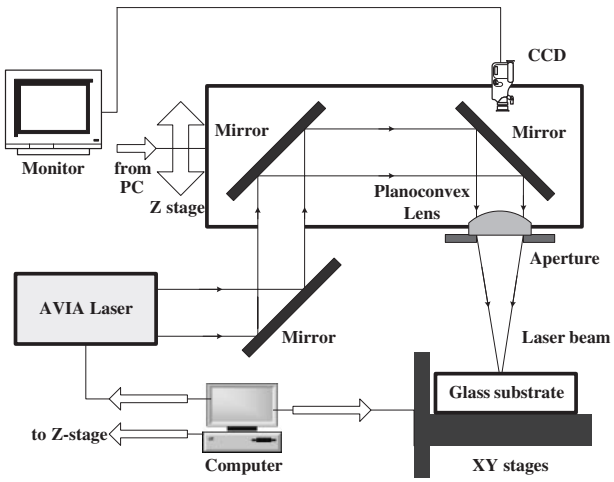

Fig. 1. Experimental setup for DPSS Nd:YAG laser (355 nm, 30 ns) microfabrication of glass substrate.

*E-mail address: HONG_Minghui@dsi.a-star.edu.sg

laser can deliver a pulse energy of up to 250 μJ at a repetition rate of 1 kHz. It offers high pulse repetition rates ranging from 1 kHz to 65 kHz that offset its low overall power. The repetition rate was set to 5 kHz for glass microfabrication. The laser beam was focused by a Plano convex lens with a focal length of 50 mm. The sample was put on a two-dimensional translation stage (Newport ALS2003-M-10-LN30AS-NC) with its surface perpendicular to the incident laser beam. The focus lens was mounted on a *Z*-direction stage (Newport ATS20020-M-40P-NC-BRK23). Vertical travel was used to determine proper focus on the sample surface. All the experiments were performed by focusing the laser beam on the front surface of the glass (spot size = 15 μm). Since most of our experiments are performed at a very low pulse energy, a broadband power meter (MELLES GRIOT BPEM001) with a resolution of 0.01 mW was used to measure output power, with the laser pulse energy being calculated as the ratio of the measured result to the repetition rate. Laser fluence (pulse energy per irradiated area) could be tuned in the range from 0.03 to 132.3 J/cm^2. The 3D stages were controlled by a computer. CAM software (MASTERCAM V9.0) was used to design the microstructures with the speed-controlled laser scanning path.

Laser ablation was carried out on lime sodium glass sheets with thicknesses of 100 μm and 700 μm. The samples were rinsed in acetone and deionized water before and after laser ablation. The widths and depths of the samples were measured from the cross-sectional view of the profile under an optical microscope (Olympus Metallurgical BH2). The cracks formed around the ablated edge were measured in size from optical images. Crack sizes at different parameters were defined as the maximum lateral length of visible damage from the ablated edge. The surface quality after laser irradiation was also observed by scanning electron microscopy (SEM, Hitachi S-4100).

3. Results and Discussion

The term pocket is used in CAM software as the use of an overlapped scanning path to scan inside a specific area. The schematic drawings of laser direct scanning and pocket scanning are shown in Fig. 2. In microfabrication, the direct method involves scanning the laser beam just along the designed structure edge, while the pocket method involves scanning a series of parallel paths with desired overlapping; either the first path or the last path can be used to form the edge of the structure. A selected number of parallel paths are defined as one loop for pocket scanning. Therefore, direct scanning can be considered as a special case of pocket scanning with only one single path in a loop. The sequent loops repeat along the same paths.

Figure 3 shows the optical image of laser scanning results on the glass surface obtained by the methods mentioned above. The laser fluence was 35.7 J/cm^2 and the scanning speed was 0.8 mm/s. A trench with a width of 15 μm was fabricated by direct scanning with one loop. The edges of the trench exhibited extended splintering and cracking. The cracks were formed randomly at the rim of the trench and the maximum lateral size of the cracks was 43.4 μm. For comparison, the same laser parameters were applied to the pocket scanning fabrication. One pocket loop, consisting of

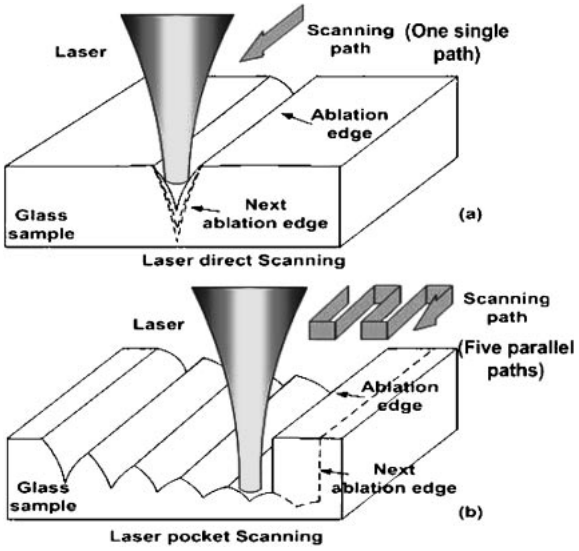

Fig. 2. Schematic drawings of (a) laser direct and (b) laser pocket scanning methods.

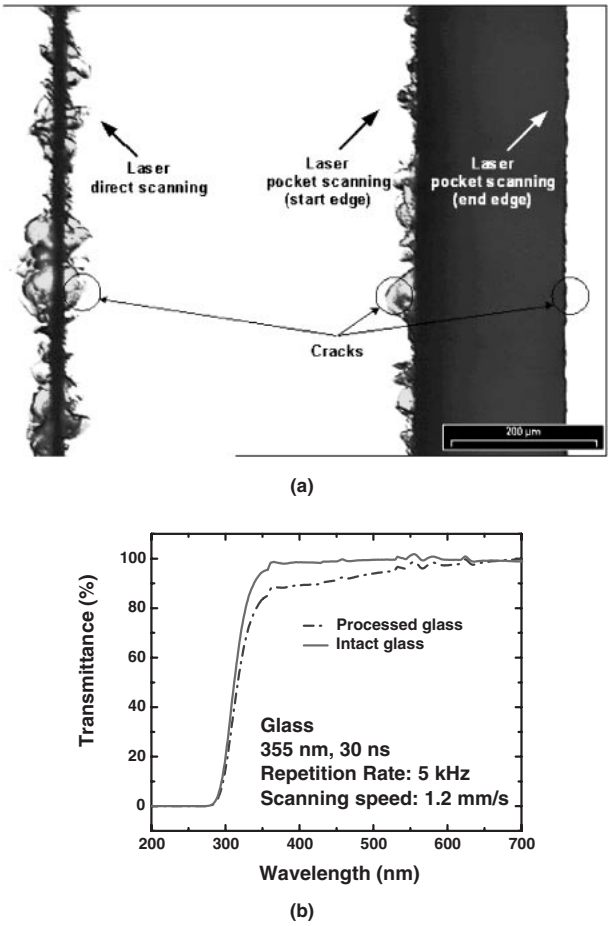

Fig. 3. (a) Optical image of trenches fabricated on glass by laser direct scanning and pocket scanning. The laser scanning speed is 0.8 mm/s at a laser fluence of 35.7 J/cm^2. The pocket scanning contains 20 parallel lines with an overlap of 5 μm in one loop (repeated loop: 1). (b) Measured transmission spectra of glass sample before and after laser direct scanning.

20 parallel paths scanning from the left to the right, was used to scan the sample surface. The distance between the centers of two parallel paths was set to 10 μm. Since the width of the

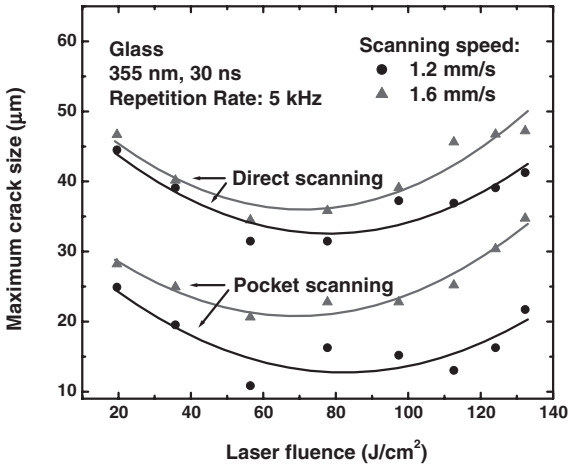

Fig. 4. Dependence of crack size on laser fluence for direct scanning and pocket scanning (repeated loop: 1) at scanning speeds of 1.2 mm/s and 1.6 mm/s.

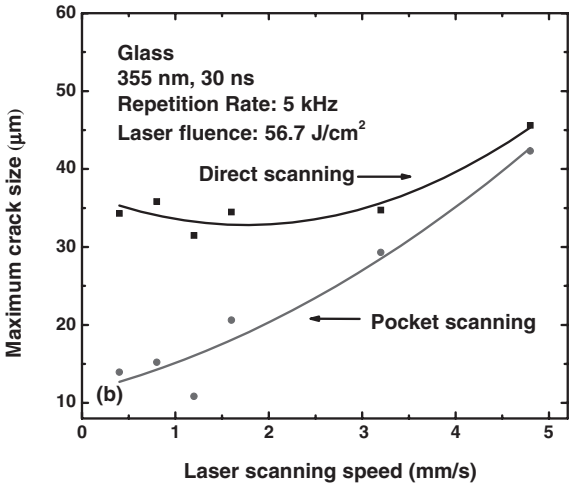

Fig. 5. Dependence of maximum crack size on laser scanning speed for laser direct scanning and pocket scanning (repeated loop: 1) at a laser fluence of 56.7 J/cm^2.

directly formed trench was 15 μm, the overlapping of the adjacent trenches in the pocket scanning was 5 μm (overlapped 33%). There were significantly different morphologies for the starting edge and the end edge. At the starting edge formed by the first path, the sizes of the cracks formed were almost the same as those in the case of the direct scanning. This is because the same processing parameters were applied. In contrast, the sizes of the cracks are reduced markedly at the end edge, and the crack distribution on laser incident side is more uniform than that on the opposite side. The improvement of the crack condition at the end edge may lead to the realization of high-quality glass structures. In the following paragraphs, the cracks generated in the pocket scanning will be specified as those formed at the end edge.

Figure 4 shows crack size as a function of laser fluence for the direct scanning and pocket scanning. The laser scanning speeds were 1.2 and 1.6 mm/s, respectively. In the pocket scanning, one loop of 10 parallel paths with an overlap of 5 μm was scanned on the sample surface. It is found that, in the direct scanning, the crack sizes are in the range from 30 μm to 50 μm, while in the pocket scanning the crack sizes are greatly reduced, with most of them being less than 30 μm. The minimum crack size appears at a laser fluence of 56.7 J/cm^2. As laser fluence increases from 19.8 to 56.7 J/cm^2, for a scanning speed of 1.2 mm/s, the crack size decreases from 44.5 to 31.5 μm for the direct scanning, and from 24.9 to 10.8 μm for the pocket scanning. When the laser fluence is higher than 56.7 J/cm^2, crack size increases accordingly. For different scanning speeds of 1.2 and 1.6 mm/s, it is also found that the lower the scanning speed, the smaller the cracks for both methods.

The detailed examination of crack size in terms of laser scanning speed was carried out, and the results are shown in Fig. 5. The scanning speeds were varied from 0.4 to 4.8 mm/s at a critical laser fluence of 56.7 J/cm^2. The parameters of the pocket scanning (10 parallel paths, 5 μm overlap) were the same as the previous ones. It is obvious that with increasing scanning speed, the cracks formed by both the direct scanning and pocket scanning increase in size. It is also found that the increase in crack size for the pocket scanning is even more rapid than that for the direct scanning. At a high scanning speed of 4.8 mm/s, the crack sizes are nearly the same for these two methods. This indicates that a lower scanning speed should be desired for reducing crack size for the pocket scanning.

It is generally understood that the formation of cracks is due to the thermal effect in nature. The irradiated laser pulses provide the glass with photonic energy, and the excited electrons dissipate excess energy into the lattice by generating phonons. For a laser pulse duration in the nanosecond range, heat transfer from hot electrons to the lattice plays a significant role in increasing lattice temperature, subsequently generating thermally induced stresses. The extended cracks in the vicinity of the formed edge indicate that thermal stress dominates in ablation.[10] The lime sodium glass used in the experiment has many defect levels due to the presence of defects and impurities. The measured transmission spectrum, as shown in Fig. 3(b), reveals that glass does not effectively absorb 355 nm laser energy via linear absorption at low laser fluences. However, as laser fluence increases, new defect levels could be generated and nonlinear (*e.g.* multiphoton) absorption could also take place, which can induce the effective deposition of laser energy into the material. Material ablation occurs when electrons are excited sufficiently to ionize atoms or molecules. However, due to the poor thermal conductivity and optical absorption of glass, a portion of the energy of glass is dissipated to nearby regions. Ablation and heat-induced stress take place simultaneously and result in crack formation around the ablated trench in the direct scanning. In the case of the pocket scanning, the laser after the first path scanning irradiates on the surface where the cracks are already formed by the previous scanning. The presence of cracks can increase the local field intensity by a factor of η^4 for transparent materials, where η is the refractive index.[11] As a result, efficient laser ablation will occur due to the very high extent of absorption in the defect regions, and thermal stress is reduced corresponding to a low heat diffusion energy. Therefore, the cracks generated from the subsequent scanning are smaller than the initial ones so as to form a sharp ablation edge.

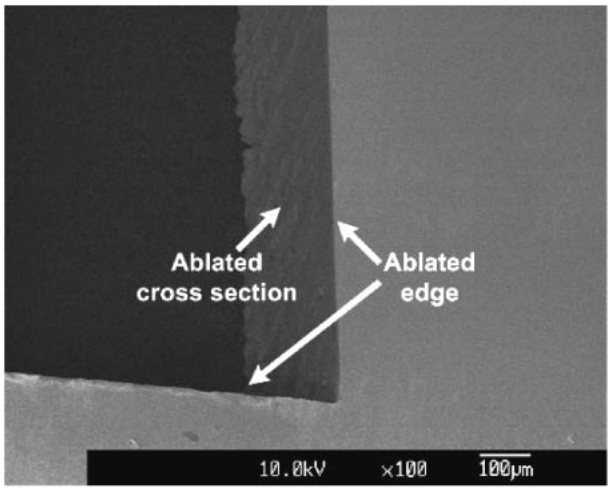

Fig. 6. SEM image of glass microstructure fabricated by pocket scanning (repeated loops: 15) at a laser fluence of 56.7 J/cm^2 and a scanning speed of 1.2 mm/s.

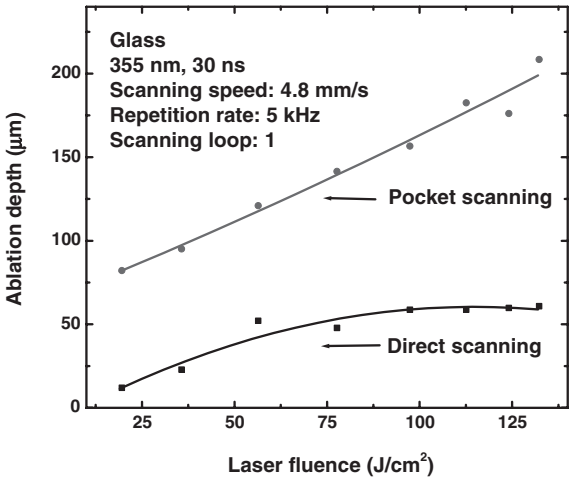

Fig. 7. Ablation depth versus laser fluence for direct scanning and pocket scanning (repeated loop: 1). The laser scanning speed is 4.8 mm/s.

The minimum crack size at an intermediate fluence could be attributed to the variation in laser energy deposition rate at different laser fluences. Another possible mechanism is the generation of shock wave and breakdown plasma during nanosecond laser ablation. Such processes take place at a high laser fluence to cause fractures in the vicinity of the interaction zone.[12] Further investigations are needed to clarify the underlying physical mechanisms of minimum crack formation. The minimum crack size could be further reduced by femtosecond laser ablation in which the heat effect is significantly minimized.[13] The increase in crack size with scanning speed could be associated with the decrease in the extent of pulse overlap. As discussed above, there is a critical laser fluence of 56.7 J/cm^2 where minimum energy contributes to heat diffusion, thereby causing cracks. As scanning speed increases, a low laser fluence indicates that crack size also increases accordingly.

In Fig. 5, it can be observed that when the scanning speed was less than 1.2 mm/s, crack size does not decrease much at a low scanning speed. A speed of 1.2 mm/s can be used as one of the optimized fabrication parameters. Figure 6 shows the SEM image of the glass microstructure fabricated using a laser fluence of 56.7 J/cm^2, a scanning speed of 1.2 mm/s and 10 parallel paths with an overlap of 5 μm. Fifteen repeated loops were used to cut through a 700 μm glass substrate with high-quality edges. The cracks around the edge are less than 10 μm. The ablated sidewall is very smooth and is vertical to the surface; no obvious slope is observed. There are some cracked edges on the rear side of glass. This may be due to the laser cutting through the glass substrate, and suddenly ejecting materials that fracture the neighboring edge, thereby causing cracks. Further improvement of edge quality may be achieved by fabricating microstructures with a protective layer such as the photoresist on the rear side.

Fabrication depth is another important parameter needed to be considered. Figure 7 shows laser ablation depth as a function of laser fluence at a scanning speed of 4.8 mm/s for the direct scanning and pocket scanning. For the pocket scanning, 10 parallel paths were used at different laser fluences. The ablation depth of glass increases from 12 to 61 μm for the direct scanning, while from 82 to 208 μm for the pocket scanning, as laser fluence increases from 20 to 132.3 J/cm^2. It is clear that the ablation depth is much higher for the pocket scanning than for the direct scanning. It can also be observed from Fig. 7 that the ablation depth for the direct scanning saturates at 50 μm at a laser fluence above 100 J/cm^2; while for the pocket scanning, the ablation depth increases almost linearly with laser fluence. The removal of substrate material is attributed to the overlapped scanning and increased light absorption of laser energy at the crack area. Furthermore, the enlarged width of the ablated trench also leads to the increase in ablation depth in the pocket scanning. The more debris generated during laser ablation, the easier it is for the debris to be ejected out of the ablated trench. A low amount of debris accumulated around the trench provides much stronger laser interaction with the glass substrate in ablation than in the direct scanning.

Figure 8 presents the ablation depth versus scanning loops at a laser fluence of 132.3 J/cm^2, an overlap of 5 μm and a scanning speed of 4.8 mm/s. It is found that the ablation depth of the pocket scanning increases almost linearly at

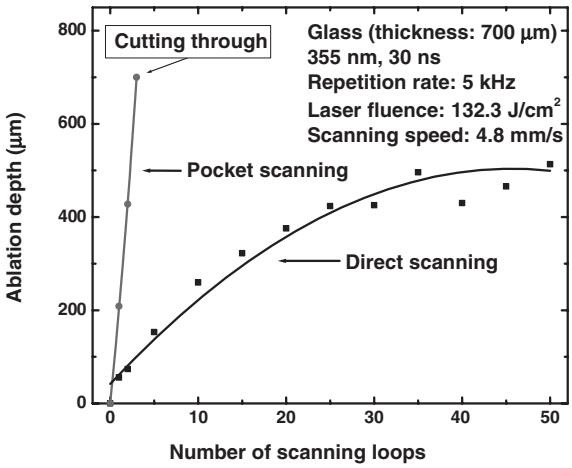

Fig. 8. Ablation depth versus number of scanning loops for direct scanning and pocket scanning. (Glass thickness: 700 μm, laser scanning speed: 4.8 mm/s and laser fluence: 132.3 J/cm^2).

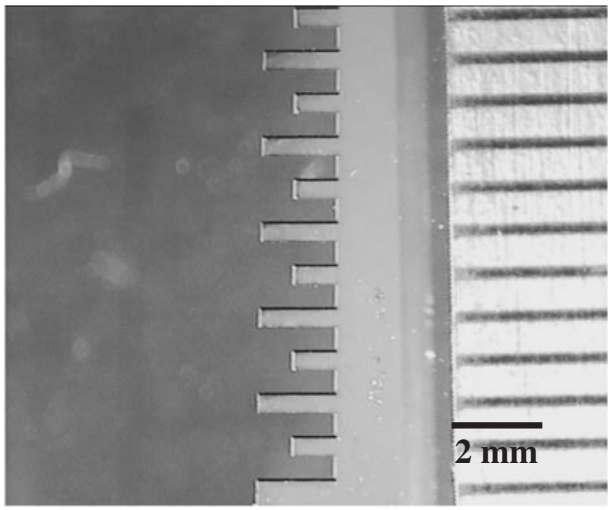

(a)

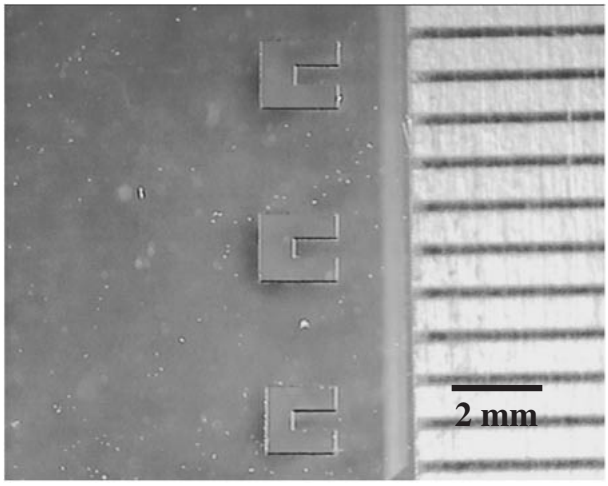

(b)

Fig. 9. Photographs of glass microstructures (thickness: 100 μm) fabricated by pocket scanning (repeated loops: 3) with optimized parameters of laser fluence of 56.7 J/cm^2 and scanning speed of 1.2 mm/s.

220 μm/loop. Three loops of the pocket scanning can cut through the 700 μm glass substrate. For the direct scanning, the ablation depth starts to saturate at 450 μm after 25 loops. It was also found in the figure that even 50 loops of the direct scanning cannot cut through this glass sheet. The saturation of ablation depth is mainly due to the accumulation of the ablated debris, which limits further laser interaction with the glass substrate. The wide trench fabricated in the pocket scanning allows the ablated materials to be ejected out of the trench more easily since the nearby area has already been ablated away. The ablation depth for the pocket scanning thus increases markedly.

The high ablation efficiency and the good control of edge quality make the pocket scanning technique a promising method for the precise engineering of glass. Figures 9(a) and 9(b) demonstrate the capabilities of the laser pocket scanning to generate arbitrary contours on the glass sheets with a thickness of 100 μm. 200-μm-width cantilevers with crack sizes less than 10 μm were fabricated at a laser fluence of 56.7 J/cm^2, a laser scanning speed of 1.2 mm/s with an overlap of 5 μm and a scanning loop of 3. Further deposition of a thin layer of piezoelectric materials or a metallic thin film with a counter electrode can make the cantilever function as an inertial sensor.[14)]

4. Conclusions

The feasibility of glass microfabrication using the DPSS Nd:YAG laser (355 nm, 30 ns) was investigated. The results show that severe cracks can be develop on glass during laser ablation by the direct scanning. Pocket scanning was employed to scan the laser beam along parallel overlapped paths with the last path forming the microstructure edge. It was found that by the pocket scanning, the cracks around the structure edges can be significantly reduced in size 2–5 μm. Crack size is minimized at a critical laser fluence and increases with laser scanning speed. Ablation depth also increases without saturation in the direct scanning. The smaller cracks size and a higher ablation depth for the pocket scanning is attributed to the high optical energy absorption in the defect regions. The wide trench fabricated by the pocket scanning also causes the ablated materials to be ejected more easily thereby increasing the ablation depth. The optimized processing parameters of a laser fluence of 56.7 J/cm^2, a laser scanning speed of 1.2 mm/s and 10 parallel paths with an overlap of 5 μm were applied to fabricate high-quality glass microstructures with crack sizes less than 10 μm.

1) E. Belloy, A. Sayah and M. A. M. Gijs: Sens. Actuat. **86** (2000) 231.
2) H. K. Tonshoff, F. V. Alvensleben, A. Ostendorf, G. Willmann and T. Wagner: Proc. SPIE **3680** (1999) 536.
3) B. Braren and R. Srinivasan: J. Vac. Sci. Technol. B **6** (1987) 537.
4) G. Markillie, H. Baker, F. Villarreal and D. Hall: Appl. Opt. **41** (2002) 5660.
5) K. Zimmer, A. Braun and R. Bohme: Appl. Surf. Sci. **208** (2003) 199.
6) J. Zhang, K. Sugioka and K. Midorikawa: Appl. Phys. A **67** (1998) 499.
7) P. R. Herman, K. Bechley, B. Jackson, K. Kurosawa, D. Moore, T. Yamanishi and J. H. Yang: Proc. SPIE **2992** (1997) 86.
8) M. Lenzner, J. Kruger, W. Kautek and F. Krausz: Appl. Phys. A **68** (1999) 369.
9) P. Rudolph, J. Bonse, J. Kruger and W. Kautek: Appl. Phys. A **69** (1999) 763.
10) J. Zhang, K. Sugioka and K. Midorikawa: Appl. Phys. A **69** (1999) 879.
11) B. C. Stuart, M. D. Feit, A. M. Rubenchik, B. W. Shore and M. D. Perry: Phys. Rev. Lett. **74** (1995) 2248.
12) M. R. Kasaai, V. Kacham, F. Theberge and S. L. Chin: J. Non-Cryst. Solids **319** (2003) 129.
13) F. Korte, S. Nolte, B. N. Chichkov, T. Bauer, G. Kamlage, T. Wagner, C. Fallnich and H. Welling: Appl. Phys. A **69** (1999) S7.
14) E. Belloy, S. Thurre, E. Walckiers, A. Sayah and M. A. M. Gijs: Sens. Actuat. A **84** (2000) 330.